IJCRT.ORG ISSN : 2320-2882

INTERNATIONAL JOURNAL OF CREATIVE RESEARCH THOUGHTS (IJCRT)

An International Open Access, Peer-reviewed, Refereed Journal

First Principal And Finite Element Simulation Of Cumno2 (With Al And Mg Doping) For Energy Storage In Supercapacitors

[1]Tikam C. Soni, [2]M. K. Manoj, [3]Mohan L. Verma, [4]M. K. Tripathi

[1]Research Scholar, [2]Assistant Professor, [3]Professor, [3]Associate Professor

[1,2,4]Department of Metallurgical and Materials Engineering, NIT Raipur, 492010, India,

[3]Department of Applied Physics, Shri Shankaracharya Technical Campus, Bhilai, 490020, India

Abstract: Supercapacitors (SCs) have gained significant attention as essential components of advanced energy storage systems, complementing renewable energy technologies and lithium-ion batteries. This study focuses on improving the performance of supercapacitors by investigating $MnCuO_2$, a transition metal oxide, doped with aluminum (Al) and magnesium (Mg). The influence of doping on the material's structural, electronic, and electrochemical properties is comprehensively analyzed using first-principles Density Functional Theory (DFT) and Finite Element Method (FEM)-based simulations. DFT calculations reveal that doping alters the crystal structure, bonding networks, and density of states, enhancing the electronic properties and stability of $MnCuO_2$. FEM simulations in COMSOL Multiphysics model the supercapacitor's performance under cyclic charging and discharging conditions. The findings establish that doping $MnCuO_2$ with Al and Mg improves specific capacitance, charge transport, and cycling stability, making it a promising electrode material for next-generation supercapacitors. This integrated computational approach provides a framework for the rational design of high-performance energy storage materials, with potential applications in sustainable energy systems.

Index Terms - Supercapacitor, Machine Learning, Simulation, First principal

1.INTRODUCTION

Supercapacitors (SCs) have emerged as a critical technology for electrochemical energy storage, complementing renewable energy systems and lithium-ion batteries[1]. They are particularly suitable for applications demanding high power density, rapid charge-discharge cycles, and extended operational lifespans[2] [3]. Based on the electrode materials used, supercapacitors are classified into three categories: Electrochemical Double-Layer Capacitors (EDLCs), Pseudocapacitors, and Hybrid Supercapacitors, which integrate the properties of both[4–6].

EDLCs rely on carbon-based materials like graphene and carbon nanotubes (CNTs), storing charge through non-faradaic processes at the electrode-electrolyte interface. Pseudocapacitors, in contrast, involve faradaic charge transfer and utilize materials such as metal oxides and conducting polymers[4]. These materials contribute to higher energy storage but vary in performance due to their distinct electrochemical and structural characteristics. Combining carbon-based materials with conducting polymers and metal oxides has proven to be an effective strategy for enhancing the overall performance of supercapacitors, enabling improved capacitance, conductivity, and stability[7].

$CuMnO_2$, a transition metal oxide, stands out as a promising electrode material for supercapacitors. Its unique crystal structure and electronic properties make it suitable for high-performance energy storage[8]. However, the inclusion of dopants like aluminum (Al) and magnesium (Mg) offers a pathway to further enhance its electrochemical characteristics by altering its electronic density of states, charge transport behavior, and

structural stability[9]. The interplay of these factors plays a crucial role in determining the material's specific capacitance, conductivity, and long-term cycling stability[10, 11].

To comprehensively understand and predict the behavior of such doped systems, advanced computational tools such as Density Functional Theory (DFT) and Finite Element Method (FEM) simulations have become indispensable[12, 13]. While DFT provides insights into the fundamental electronic and structural properties, FEM enables the modeling of device-scale phenomena, such as charge transport and electric potential distribution, under realistic operating conditions[14]. Furthermore, the incorporation of machine learning techniques into materials research facilitates the rapid screening and optimization of promising compositions, accelerating the discovery of next-generation energy storage materials.

In this work, we investigate the structural, electronic, and electrochemical properties of $CuMnO_2$ doped with Al and Mg using a combination of first-principles DFT calculations and FEM-based simulations. The influence of doping on the crystal structure, density of states, and charge storage behavior is analyzed, providing a holistic understanding of its potential for supercapacitor applications. The FEM simulations conducted using COMSOL Multiphysics elucidate the transient response of supercapacitors under cyclic charging and discharging, offering practical insights into their performance. This integrated approach aims to establish a framework for the rational design of high-performance materials for energy storage technologies.

2. METHODS

2.1 Density functional Theory Calculation

The first-principles calculations were performed using the SIESTA (Spanish Initiative for Electronic Simulations with Thousands of Atoms) package[15]. The crystallographic information files (CIFs) for MnCuO2, MnAlCuO2 and MnAlCuO2 were obtained from the Materials Project database, with structures corresponding to their respective space groups. The Perdew-Burke-Ernzerhof (PBE) scheme within the framework of the Generalized Gradient Approximation (GGA) was used as the exchange-correlation functional for structural optimization and electronic property calculations. The structural optimization was performed using the conjugate-gradient (CG) technique, with energy minimization carried out until the forces on each atom were less than 0.001 eV/Å and the energy convergence reached 0.0001 Ry. A U value of 4 eV was used, consistent with previous studies on similar compounds. This method ensured a more accurate representation of the electronic structure and density of states.

2.2 FEM simulation in COMSOL

The performance of the supercapacitor was modeled using COMSOL Multiphysics. A 2D cross-sectional model was created with symmetric geometry, representing the supercapacitor's structure. The model included the central region for the electrolyte and separator and the outer regions corresponding to the anode and cathode. Triangular meshing was applied to ensure computational accuracy, as shown in Figure 3[16].

The simulation parameters used for the study are summarized in Table 2. These include the geometric dimensions of the electrodes, electrolyte, and separator, as well as the electrical conductivities of the materials. Key parameters include a cathode and anode length of 150 µm, an electrolyte thickness of 100 µm, and conductivities of 6.5 S/m for the electrolyte and 0.01 S/m for the electrodes.

The electric potential distribution across the supercapacitor was simulated, as shown in Figure 4. The color gradient in the results depicts the electric potential, with higher values near the cathode (red) and lower values near the anode (blue). The arrows represent the vector field of the current density, with direction and magnitude indicating charge transport behavior.

A transient study was conducted to analyze the supercapacitor's electrochemical performance under cyclic charging and discharging conditions. The results, illustrated in Figure 5, include the time-dependent cell potential and current. The potential oscillates between 0 V and 2.6 V, showing a nearly linear trend typical of capacitive behavior. The current alternates between +0.01 A and -0.01 A, following a square-wave profile, indicating periodic charge and discharge cycles. The smooth curves demonstrate stable and controlled operation, providing insight into the supercapacitor's performance.

3. RESULTS AND DISCUSSION

3.1 Crystal Structure configurations of MnCuO2 with Al, Mg doping

Figure 1 depicts crystal structures for different configurations of MnCuO2 with Al, Mg doping. The structures highlights interactions or bonding between various elements. Figure 1(a) shows an interaction between manganese (Mn), copper (Cu), and oxygen (O) atoms. It forms a framework with Mn1 and Mn2 connected to oxygen atoms (O7 and O5) and Cu atoms (Cu3 and Cu4). The oxygen atoms at the base (O6 and O8) are terminating or connected to another system. Figure 1(b) adds aluminum (Al1) to the system, replacing Mn1 in Figure 1(a). The Al atom forms bonds with oxygen atoms (O7 and O5), connected to copper atoms (Cu3 and Cu4). This structure shows an alternative configuration with aluminum interacting within a Mn-Cu-oxide framework, emphasizing changes in the material's properties due to the substitution of Al. Figure 1 (c) has magnesium (Mg1) replaces Mn1 or Al1 in the previous structures, interacting with Mn2, copper (Cu3 and Cu4), and oxygen atoms (O7 and O5). This configuration represents another substitution or doping scenario, to study the influence of magnesium on the material's structure and properties. The substitution or doping of these elements impacts the electronic, structural, or electrochemical properties of the material which is relevant in fields of energy storage.

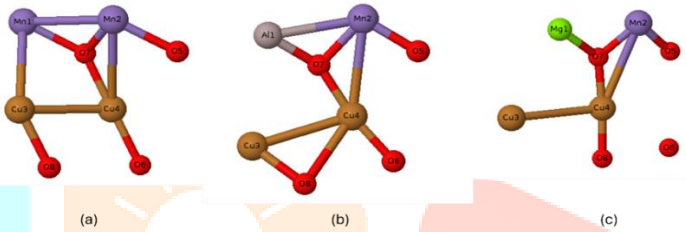

Figure 1 Optimized Crystal Structure of (a) MnCuO2 (b) MnCuO2 with Al and (c) MnCuO2 with Mg

3.2 Density of states for MnCuO2 with Al, Mg doping

Figure 2 compares the density of states (DOS) for two materials: MnCuO2 (a) and MnAlCuO2 (b). Both graphs plot the DOS as a function of energy, with the Fermi level located at E=0. In MnCuO2, the DOS shows prominent peaks below the Fermi level (in the negative energy region) around -4 eV and -2 eV, suggesting the presence of significant electronic states from occupied orbitals. Above the Fermi level, the DOS decreases, indicating fewer available states in the conduction band. In contrast, MnAlCuO2 exhibits a similar general shape but displays sharper and more defined peaks around -4 eV and -2 eV, possibly due to the addition of aluminum altering the electronic structure. The peaks are also slightly shifted, which may indicate a modification in the bonding and orbital contributions. Overall, the inclusion of aluminum appears to affect the electronic states, potentially enhancing the material's electronic properties, such as its conductivity or catalytic activity.

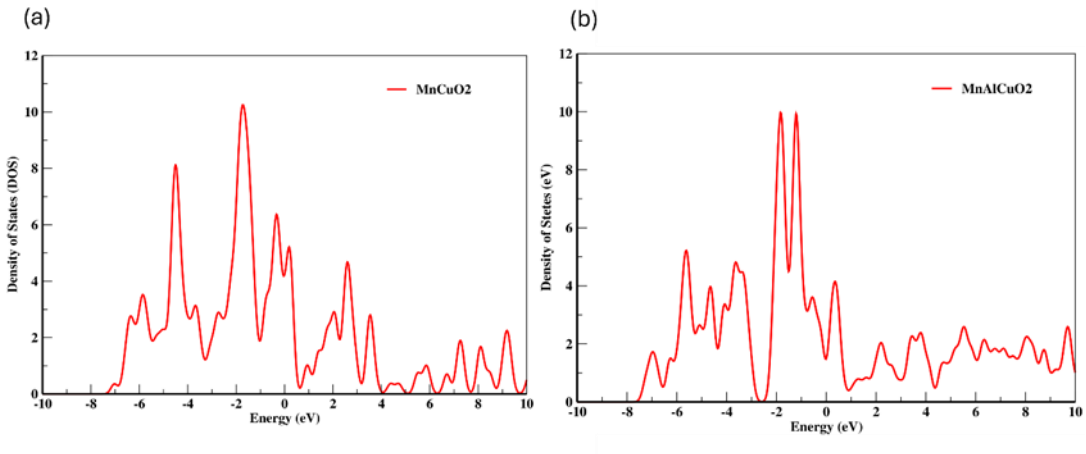

Figure 2 Density of States (DOS) for MnCuO2 (a) and MnAlCuO2 (b), highlighting the influence of aluminum substitution on the electronic structure near the Fermi level.

3.3 COMSOL simulation Results

Figure 3 represent the meshing of a model in COMSOL Multiphysics for the supercapacitor simulation. It shows a 2D or cross-sectional triangular mesh applied to supercapacitor geometry. The central region represents the electrolyte and separator and the outer regions on both the sides correspond to the electrodes. The geometry and meshing are symmetric about the vertical axis, typical for supercapacitor models assuming a uniform or symmetric design.

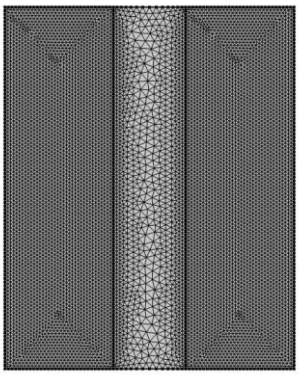

Figure 3 Triangular Meshing of supercapacitor model

Table 2 Shows the parameters used in the COMSOL Simulation which summarizes the geometrical and material parameters used in the COMSOL simulation to model the supercapacitor.

Table 2: COMSOL Simulation Parameters

Symbol	Value	Details
r_in	0.1[mm]	Inner radius
l_c	150[um]	Cathode length
l_a	150[um]	anode length
l_e	100[um]	electrolyte
h_cap	500[um]	Height of supercapacitor
sigma_e	6.5[S/m]	Conductivity of electrolyte
sigma_a_c	.01[S/m]	Conductivity of Anode Cathode

Figure 4 represents the results of a COMSOL simulation for a supercapacitor, showing the distribution of electric potential across the device. The color gradient indicates the variation in electric potential across the supercapacitor. The red regions signify higher values, likely near the cathode, while the blue regions represent lower values, possibly near the anode. The central gradient (from red to blue) corresponds to the electrolyte region, where the field or charge transfer occurs between the electrodes. The arrow directions indicate the flow direction of field, while the arrow length or density represent the magnitude.

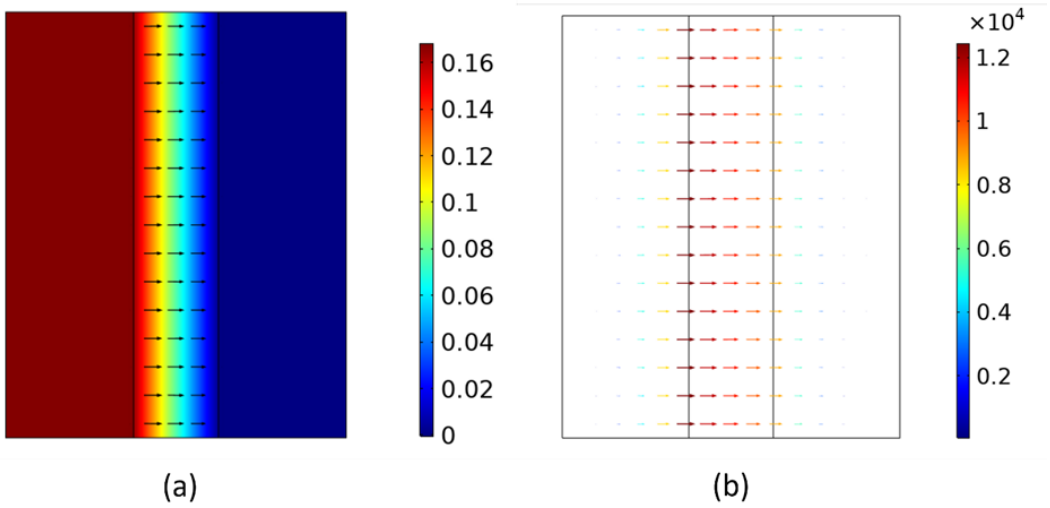

Figure 4 Spatial distribution of the electric potential (a) and the corresponding vector field of current density (b) across the electrodes and electrolyte

Figure 5 show results from a COMSOL simulation of a supercapacitor's performance under specific operating conditions. Transient study or electrochemical analysis, displaying the behavior of the cell potential (voltage) and cell current over time. The cell potential oscillates between approximately 0 V and 2.6 V. The periodic behavior suggests that the system might be subjected to cyclic charging and discharging, typical in supercapacitor analysis. The smooth nature of the curve indicates controlled charge and discharge cycles without significant instability. The current oscillates between approximately +0.01 A and -0.01 A. The periodic, sharp transitions indicate alternating charge and discharge currents applied to or drawn from the supercapacitor. The potential ramps up during charging and decreases during discharging, following a nearly linear trend (suggesting a capacitive behavior typical of supercapacitors). The square-wave current profile aligns with a charge-discharge cycling setup where constant current is applied.

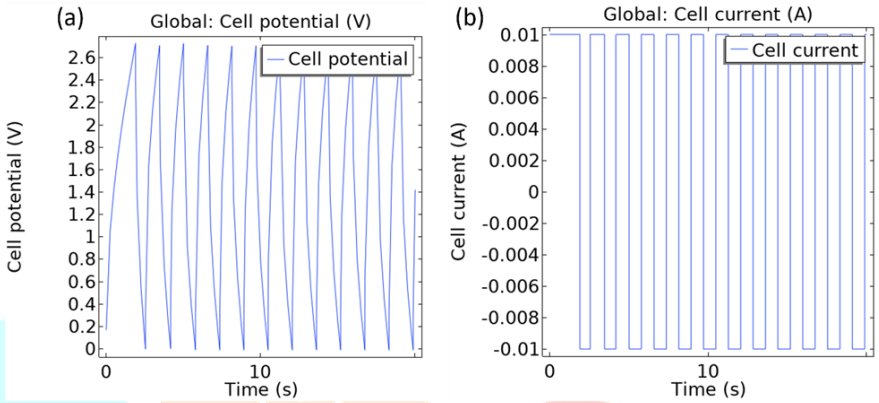

Figure 5 Transient study (a) Cell Potential and (b) Cell current over time

4. CONCLUSION

This study investigates the structural, electronic, and simulation-based properties of $MnCuO_2$ doped with aluminum (Al) and magnesium (Mg), with a focus on their potential applications in energy storage devices like supercapacitors. The crystal structure analysis reveals how the substitution of Mn with Al and Mg alters the bonding network, providing insights into the material's stability and performance. The density of states (DOS) analysis shows that doping with aluminum shifts the electronic structure, potentially enhancing the material's electronic properties such as conductivity, which is beneficial for energy storage applications.
Furthermore, the COMSOL simulations highlight the design and performance of a supercapacitor model, showing the distribution of electric potential and current density within the device. The symmetric meshing and the simulation results emphasize how the material's properties can be optimized for better energy storage performance. Overall, the findings suggest that doping $MnCuO_2$ with Al and Mg can significantly modify its structural and electronic properties, making it a promising candidate for improving the efficiency of supercapacitors and other energy storage technologies. Future work could focus on experimentally validating these simulations and exploring other doping elements for further enhancement of performance.

ACKNOWLEDGMENT

This research is supported by the National Institute of Technology Raipur, Chhattisgarh, India. The Ministry of Human Resources and Development (MHRD) of India has provided funding in the form of a fellowship has been greatly acknowledge.

REFERENCES

[1] Conway BE. 1991. Transition from "Supercapacitor" to "Battery" Behavior in Electrochemical Energy Storage. J Electrochem Soc 138(6):1539–1548.

[2] Nohara S, Wada H, Furukawa N, Inoue H, Morita M, Iwakura C. 2003. Electrochemical characterization of new electric double layer capacitor with polymer hydrogel electrolyte. Electrochimica Acta 48(6):749–753.

[3] Conway BE, Pell WG. 2003. Double-layer and pseudocapacitance types of electrochemical capacitors and their applications to the development of hybrid devices. J Solid State Electrochem 7(9):637–644.

[4] Shao Y, El-Kady MF, Sun J, Li Y, Zhang Q, Zhu M, Wang H, Dunn B, Kaner RB. 2018. Design and Mechanisms of Asymmetric Supercapacitors. Chem Rev 118(18):9233–9280.

[5] Miller JM, Dunn B, Tran TD, Pekala RW. 1997. Deposition of Ruthenium Nanoparticles on Carbon Aerogels for High Energy Density Supercapacitor Electrodes. J Electrochem Soc 144(12):L309–L311.

[6] Yang Q, Li Q, Yan Z, Hu X, Kang L, Lei Z, Liu Z-H. 2014. High performance graphene/manganese oxide hybrid electrode with flexible holey structure. Electrochimica Acta 129:237–244.

[7] Afif A, Rahman SM, Tasfiah Azad A, Zaini J, Islan MA, Azad AK. 2019. Advanced materials and technologies for hybrid supercapacitors for energy storage – A review. J Energy Storage 25:100852.

[8] Bahmani F, Kazemi SH, Wu Y, Liu L, Xu Y, Lei Y. 2019. CuMnO2-reduced graphene oxide nanocomposite as a free-standing electrode for high-performance supercapacitors. Chem Eng J 375:121966.

[9] Kurokawa A, Yanoh T, Yano S, Ichiyanagi Y. 2014. Preparation and Magnetic Properties of Multiferroic CuMnO 2 Nanoparticles. J Nanosci Nanotechnol 14(3):2553–2556.

[10] Bahmani F, Kazemi SH, Wu Y, Liu L, Xu Y, Lei Y. 2019. CuMnO2-reduced graphene oxide nanocomposite as a free-standing electrode for high-performance supercapacitors. Chem Eng J 375:121966.

[11] Ashourdan M, Semnani A, Hasanpour F, Moosavifard SE. 2021. Synthesis of CuMnO2/graphene quantum dot nanocomposites as novel electrode materials for high performance supercapacitors. J Energy Storage 36:102449.

[12] Emery AA, Wolverton C. 2017. High-throughput DFT calculations of formation energy, stability and oxygen vacancy formation energy of ABO3 perovskites. Sci Data 4(1):170153.

[13] Xu Q, Yang GM, Zheng WT. 2020. DFT calculation for stability and quantum capacitance of MoS2 monolayer-based electrode materials. Mater Today Commun 22:100772.

[14] Beltran H, Sansano E, Pecht M. 2023. Machine learning techniques suitability to estimate the retained capacity in lithium-ion batteries from partial charge/discharge curves. J Energy Storage 59:106346.

[15] García A, Papior N, Akhtar A, Artacho E, Blum V, Bosoni E, Brandimarte P, Brandbyge M, Cerdá JI, Corsetti F, Cuadrado R, Dikan V, Ferrer J, Gale J, García-Fernández P, García-Suárez VM, García S, Huhs G, Illera S, Korytár R, Koval P, Lebedeva I, Lin L, López-Tarifa P, Mayo SG, Mohr S, Ordejón P, Postnikov A, Pouillon Y, Pruneda M, Robles R, Sánchez-Portal D, Soler JM, Ullah R, Yu VW, Junquera J. 2020. Siesta: Recent developments and applications. J Chem Phys 152(20):204108.

[16] Electrochemical Capacitor with Porous Electrodes. COMSOL. Available from https://www.comsol.com/model/electrochemical-capacitor-with-porous-electrodes-91371, [03/12/2024].